Theor Chem Acc (1999) 103:1–8
DOI 10.1007/s002149900005

Theoretical
Chemistry Accounts

Regular article

Transition states in modern valence-bond theory: application to the Cope rearrangement

Josep M. Oliva

Institut de Ciència de Materials de Barcelona, CSIC Campus de la UAB, E-08193 (Bellaterra), Spain
e-mail: jmo@kanigo.icmab.es

Received: 13 October 1998 / Accepted: 30 December 1998 / Published online: 7 June 1999

Abstract. Modern valence-bond theory, in its spin-coupled form, is used to study the electronic structure of the transition structures in the Cope rearrangement. It is found that the transition structure described by a "chair" geometry with a "6-in-6" CASSCF/6-31G* wave function is clearly aromatic while the CASSCF/6-31G* "boat" transition structure corresponds more closely to two weakly interacting allyl radicals. Moreover, there is a striking resemblance between the CASSCF chair transition structure and the benzene molecule, arising from the modern valence-bond analysis in terms of Rumer spin functions. In agreement with previous works, dynamical correlated wave functions show shorter interallylic distances in the optimized transitions structures. The use of spin-coupled wave functions on the latter geometries results in diradical and aromatic character for the chair and boat transition structures, respectively.

Key words: Valence-bond theory – Transition state – Cope rearrangement – Allyl radical – Resonance energy – Spin coupling

1 Introduction

The Cope rearrangement of 1,5-hexadiene is one of the most studied chemical reactions of the last two decades. Semiempirical, ab initio and density functional theory studies have been performed with a variety of results [1–13]. It is commonly accepted that this reaction can occur via a C_{2h} chair or C_{2v} boat transition structure (TS), the latter having a higher barrier. Whether the C_{2h} TS is of diradicaloid or aromatic nature depends on the interallylic distance at the TS. Inclusion of dynamical correlation via (truncated) multireference configuration interaction and quasidegenerate variational perturbation theory predicts a diradicaloid (cyclohexanediyl) and an aromatic TS, respectively [8].

Hrovat et al. [9] showed that there is only one (constrained) C_{2h} chair TS at the CASPT2N level of theory [10, 11] and that energy barriers agree better with experiment at this level of theory compared to the CASSCF results. Kozlowski et al. [12] also showed that the CASSCF wave function overestimates the diradical character of the chair TS. Using similar CASMP2 techniques they showed that the chair Dewar-type diradicaloid stable intermediate no longer occurs as a minimum in the potential energy surface, the aromatic chair TS moving to shorter interallylic bond lengths in agreement with the results of Hrovat et al. On the other hand, using ab initio and density functional theory techniques, Jiao and Schleyer [13] located chair and boat TSs, and calculated their magnetic properties through IGLO analysis [14], thus claiming that the rearrangement occurs through a concerted, synchronous mechanism via an aromatic TS.

In this work, we first present a valence-bond (VB) study of the chair and boat TS in the Cope rearrangement using the TS optimized geometries from nondynamical (CASSCF) and dynamical (MP4 and QCISD) correlated ab initio wave functions. The main goal of this work is not to provide an answer as to whether the Cope rearrangement of 1,5-hexadiene passes through an aromatic or a diradical TS, but rather to give a description of how modern VB wave functions can describe the aromaticity or diradical character of TSs found at different levels of theory. One of the VB methods, spin-coupled (SC) theory [15], is used for analyzing the chair and boat TS in the Cope rearrangement. A brief description of this method is given in the next section.

2 Computational approach – SC theory

The SC wave function used in this work has the form [16]:

$$\Psi_{S,M} = \sqrt{N!}\mathscr{A}\left(\psi_1^2\psi_2^2\cdots\psi_{n_c}^2\ \Theta_{S,M}^{2n_c}\ \phi_1\phi_2\cdots\phi_N\ \Theta_{S,M}^N\right)\ , \tag{2.1}$$

which corresponds to n_c doubly occupied core orbitals and N SC orbitals, respectively, with an overall spin S

and z-projection M. The SC orbitals ϕ_μ are singly occupied and non-orthogonal:

$$\langle \phi_\mu | \phi_v \rangle = \Delta_{\mu v}; \ \mu, \ v = 1, \ldots, N \ . \tag{2.2}$$

The core orbitals ψ_i can always be taken to be orthonormal to one another and orthogonal to the SC orbitals without changing the total wavefunction Ψ:

$$\langle \psi_i | \psi_j \rangle = \delta_{ij}; \quad i, j = 1, \ldots, n_c \tag{2.3}$$

$$\langle \phi_\mu | \psi_j \rangle = 0; \quad \mu = 1, \ldots, N; \ j = 1, \ldots, n_c \ . \tag{2.4}$$

The spin functions $\Theta_{S,M}^N$ and $\Theta_{S,M}^{2n_c}$ correspond to the active and core electrons, respectively, the latter being the perfectly paired spin function for $2n_c$ electrons (each of the n_c pairs coupled to a singlet). The core and SC orbitals are expanded in terms of atomic functions, much as in molecular orbital theory:

$$\psi_i = \sum_{p=1}^{m} c_{ip} \chi_p; \quad \phi_\mu = \sum_{p=1}^{m} c_{\mu p} \chi_p \ . \tag{2.5}$$

The spin function corresponding to the active orbitals is written as a linear combination of f_S^N linearly independent $N-$electron spin functions, which are eigenfunctions of $\hat{S}^2$ and $\hat{S}_z$ with eigenvalues S and M respectively:

$$\Theta_{S,M}^N = \sum_{k=1}^{f_S^N} C_{Sk} \Theta_{S,M;k}^N \ , \tag{2.6}$$

where the C_{Sk} are the spin-coupling coefficients. There are f_S^N ways of coupling N electrons to a total spin S. The value of f_S^N is given by

$$f_S^N = \frac{(2S+1)N!}{(\frac{N}{2}+S+1)!(\frac{N}{2}-S)!} \ . \tag{2.7}$$

The set of variational parameters for optimizing the energy expectation value corresponding to Ψ consists of all coefficients $c_{ip}, c_{\mu p}$ and C_{Sk} from Eqs. (2.5) and (2.6). The f_S^N spin functions $\Theta_{S,M;k}^N$ in Eq. (2.6) are not unique and different bases of spin functions are commonly used, most often the Kotani (or branching diagram, see for example, Ref. [17]), Rumer [18] and Serber [19] bases, respectively. In this work, use will be made of the Rumer spin basis. It is usual to define the Rumer spin functions as

$$R = (\mu_1\text{–}\mu_2, \mu_3\text{–}\mu_4, \ldots, \mu_{N-2S-1}\text{–}\mu_{N-2S}) \ , \tag{2.8}$$

where μ_p–μ_q corresponds to a singlet coupling between electrons μ_p and μ_q. In all, there are f_S^N linearly independent spin functions in which the first $N-2S$ electrons form singlet pairs, and the remaining $2S$ electrons are assigned spins α. Since we are interested in the ground-state singlet chemical reaction and the number of active electrons is even, the total spin S is zero and therefore each individual Rumer spin function consists of $N/2$ singlet pairs μ_p–μ_q. The weights of each spin function in an orthogonal basis such as the Kotani and Serber ones, are defined as

$$W_k = |C_{Sk}|^2 \ . \tag{2.9}$$

More generally, as in the Rumer basis, where the spin functions are not orthogonal, the weights W_k are given by

$$W_k = C_{Sk} \sum_{l=1}^{f_S^N} \Delta_{kl} C_{Sl} \ , \tag{2.10}$$

where Δ_{kl} is the overlap between spin functions R_k and R_l. As is well known Eq. (2.10), which was first introduced by Chirgwin and Coulson [20], is not the only way of defining the weight in nonorthogonal bases; Gallup and Norbeck [21] also defined weights which also satisfy (as Eq. 2.10 does)

$$\sum_{k=1}^{f_S^N} W_k = 1 \ . \tag{2.11}$$

In this work, we use the weights defined by Chirgwin and Coulson [20], since comparisons will be made between these weights in the Cope TSs and those arising from the benzene molecule. The VB interpretation of the SC wave function involves solving the secular equation [22]

$$\sum_J (H_{IJ} - E\Delta_{IJ}) C_J = 0 \ , \tag{2.12}$$

where $H_{IJ} = \langle \Phi_I | \mathscr{H} | \Phi_J \rangle$ and $\Delta_{IJ} = \langle \Phi_I | \Phi_J \rangle$ are the matrix elements of the Hamiltonian and the overlap between structures Φ_I and Φ_J, respectively. The eigenvalues (ground- and excited-state energies) of Eq. (2.12) are analyzed in terms of the Chirgwin–Coulson occupation numbers [20], defined as

$$n_I = C_I \sum_J \Delta_{IJ} C_J \ , \tag{2.13}$$

which obviously also satisfy Eq. (2.11).

3 Results and discussion

The geometries of the chair and boat TSs were optimized at the CASSCF level of theory using a 6-31G* basis set, which is of double-ζ quality and contains polarization d functions (xx, yy, zz, xy, xz, yz) on the carbon atoms [23]. An active space of six electrons in six orbitals was used in the CASSCF calculations, which are denoted as CAS(6,6)/6-31G*. The geometries of the chair and boat TSs are shown in Fig. 1 in terms of the inter-allylic distance $R_1 = R(C_1C_6) = R(C_3C_4)$, the carbon–carbon distance in each allyl fragment $R_2 = R(C_1C_2) = R(C_2C_3) = R(C_4C_5) = R(C_5C_6)$, and the angles α and β which describe, respectively, the allylic angle $\alpha = \angle C_1C_2C_3 = \angle C_4C_5C_6$ and the bending angle of each allyl fragment with respect to the plane defined by C_1, C_3, C_4 and C_6.

The point-symmetry groups (PSG) of the chair and boat TSs are C_{2h} and C_{2v}, respectively. Further CAS(6,6)/6-31G* frequency calculations at the optimized TSs were performed in order to check the number of imaginary frequencies. Thus, the chair and boat TSs showed single imaginary frequencies of $780i$ cm^{-1} (A_u symmetry) and $477i$ cm^{-1} (B_1 symmetry), respectively. Both displacements (A_u and B_1) follow a wagging

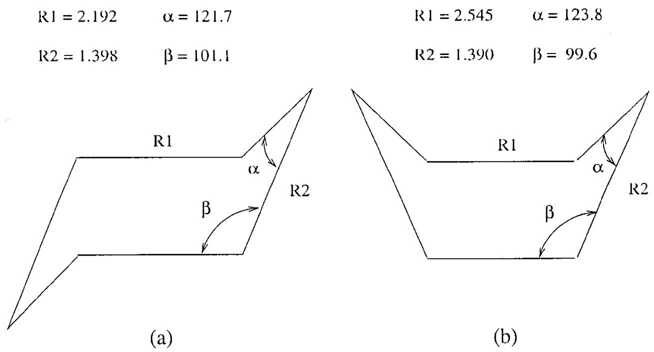

Fig. 1. Optimized geometries of **a** the chair C_{2h} and **b** the boat C_{2v} transition structures in the Cope rearrangement at the CASSCF(6,6) level using the 6-31G* basis set. Distances (R) in angstrom and angles (α, β) in degrees

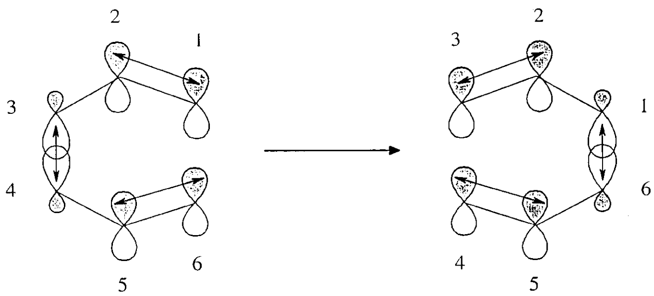

Fig. 2. Six-electron valence-bond model for the Cope rearrangement

motion of the allyl fragments approaching from one extreme ($C_1 \rightarrow\leftarrow C_6$) and being pulled apart on the other side ($C_3 \longleftrightarrow C_4$); these displacements coincide with the reaction coordinate (Fig. 1) [24]. It is important to emphasize that the symmetry of the molecule is reduced when changing the geometry of the TSs following the normal mode of the imaginary frequency:

$$\begin{aligned} &\text{Chair: } C_{2h} \rightarrow C_2 \\ &\text{Boat: } C_{2v} \rightarrow C_s \ . \end{aligned} \tag{3.1}$$

At these optimized geometries, the distance between allyl fragments in the chair and boat TSs differs by $|\Delta R_1| \sim 0.35$ Å, the other geometrical parameters being very similar: $|\Delta R_2| = 0.008$ Å, $|\Delta\alpha| = 2.1°$, and $|\Delta\beta| = 1.5°$.

Within VB theory, the Cope rearrangement of 1,5-hexadiene is simply the transformation of one VB structure into another as shown in Fig. 2. Hence in VB terms the reaction can be modelled using six active electrons: four electrons describing the two π bonds $\pi_{C_1\text{-}C_2}, \pi_{C_5\text{-}C_6}$, and two electrons corresponding to the interallylic σ bond $\sigma_{C_3\text{-}C_4}$. The recoupling of these six active electrons generates two new π bonds, $\pi_{C_2\text{-}C_3}$ and $\pi_{C_4\text{-}C_5}$, and a new σ bond, $\sigma_{C_1\text{-}C_6}$.

Using the CAS(6,6)/6-31G* optimized geometries shown in Fig. 1, SC calculations were then carried out on the chair and boat TSs. The six-active-electron model corresponding to the VB structures of Fig. 2 is then translated into SC calculations including six singly occupied non-orthogonal (SC or active) orbitals which are variationally optimized together with 20 core (doubly occupied) orbitals and the five different spin-coupling coefficients C_{0k} , $k = 1$–5 (the number of spin-coupling coefficients is given by f_S^N in Eq. 2.7). These calculations are denoted as SC(20c, 6v): The 46 electrons in 1,5-hexadiene are thus partitioned into two sets: one set of 20 optimized doubly occupied orbitals (20c) which, together with the nuclei of the molecule, describe an average potential in which the set of six (6v) active electrons move. The wavefunction SC(20c, 6v) can be written as

$$\Psi_{SC} = \sqrt{6!}\mathscr{A}\left(\psi_1^2\psi_2^2\cdots\psi_{20}^2\ \Theta_{00}^{40}\ \phi_1\phi_2\cdots\phi_6\ \Theta_{00}^6\right) \ , \tag{3.2}$$

where

$$\begin{aligned} \Theta_{00}^{40} = {} & \frac{1}{\sqrt{2}}(\alpha_1\beta_2 - \beta_1\alpha_2)\frac{1}{\sqrt{2}}(\alpha_3\beta_4 - \beta_3\alpha_4) \\ & \cdots\frac{1}{\sqrt{2}}(\alpha_{39}\beta_{40} - \beta_{40}\alpha_{39}) \ , \end{aligned} \tag{3.3}$$

corresponds to 20 pairs of electrons, each pair coupled to a singlet (perfectly paired spin function), and

$$\Theta_{00}^6 = \sum_{k=0}^{5} C_{0k}\Theta_{00;k}^6 \tag{3.4}$$

is the total spin ($S = 0$) function assigned to the six active electrons. The spin-coupling coefficients C_{0k} are not uniquely defined and depend on the spin basis used for the particular problem; however, the VB structures shown in Fig. 2 make use of the Rumer spin basis [18], which we simply label as

$$R_k = (\mu_1\text{–}\mu_2, \mu_3\text{–}\mu_4, \mu_5\text{–}\mu_6) \ , \tag{3.5}$$

where μ_p–μ_q means that electrons μ_p and μ_q are coupled to a singlet. In the SC calculations, the five Rumer structures are ordered as

$$\begin{aligned} R_1 &= (1\text{–}2, 3\text{–}4, 5\text{–}6), \\ R_2 &= (2\text{–}3, 1\text{–}4, 5\text{–}6), \\ R_3 &= (1\text{–}2, 4\text{–}5, 3\text{–}6), \\ R_4 &= (2\text{–}3, 4\text{–}5, 1\text{–}6), \\ R_5 &= (3\text{–}4, 2\text{–}5, 1\text{–}6) \ . \end{aligned} \tag{3.6}$$

Hence the Cope rearrangement of 1,5-hexadiene can be described as follows (Fig. 2):

$$R_1 \rightarrow R_4 \ . \tag{3.7}$$

In this particular case, the 6-31G* basis set corresponds to a set of 110 atomic basis functions. Therefore, the total number of variational parameters used in the SC calculations includes (110 basis functions) × (20 core + 6 active orbitals) + (5 spin-coupling coefficients) = 2865 parameters; however, not all these parameters are independent since Ψ_{SC} and each active orbital are normalized, and the core orbitals satisfy certain conditions which reduce the number of independent parameters [16]. The active orbitals also fulfil certain symmetry re-

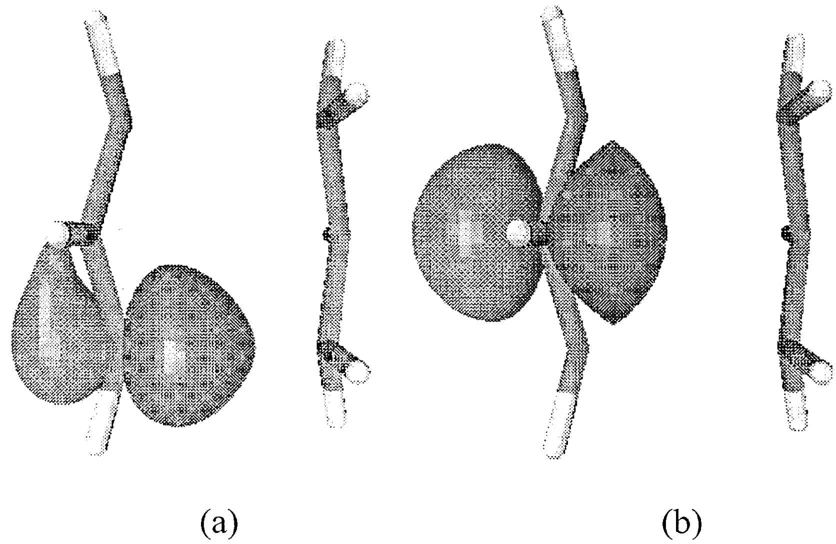

Fig. 3a, b. Symmetry-unique spin-coupled (*SC*) orbitals in the C_{2h} chair transition structure using SC(20c, 6v) wave function with the optimized geometry at the CAS(6,6)/6-31G* level of theory. **a** orbital ϕ_1 (symmetry-equivalent to ϕ_3, ϕ_4 and ϕ_6); **b** Orbital ϕ_2 (symmetry-equivalent to ϕ_5)

lations depending on the converged wavefunction; thus, one often finds that a many-electron system with a given geometry can have several close minima in the energy hypersurface of the variational parameters.

As a starting guess for Ψ_{SC} in the chair and boat TSs, we used the 20 core orbitals obtained from the Pipek–Mezey localization procedure [25]. Thus, six orbitals corresponding to the $1s^2$ core electrons on each carbon, ten localized σ_{CH} orbitals and four localized $\sigma_{C\text{-}C}$ orbitals corresponding to the four carbon–carbon bonds of the two allyl fragments which are not active in the six-electron VB model (Fig. 2), i.e., C_1-C_2, C_2-C_3, C_4-C_5 and C_5-C_6, were used as starting guesses for the optimization of the core. The initial guess for the active orbitals was simply a $+2p_z$ function centred on C_1, C_2, and C_3 and a $-2p_z$ function centred on C_4, C_5, and C_6, respectively, where the z-axis is chosen to be parallel to R_1 and bisects each allyl fragment (Fig. 1). With this initial guess, no problems were encountered in the convergence of Ψ_{SC}^{chair} and Ψ_{SC}^{boat}: both wavefunctions converged to respective minima, which were checked through the reduced Hessian matrix of the SC energy at convergence [16]. The converged symmetry-unique (SU) SC orbitals from the chair and boat TSs at the CAS(6,6)/6-31G* optimized geometries are shown in Figs 3 and 4, respectively.

The overlap integrals between the six active orbitals in the chair and boat TSs are shown in Tables 1 and 2 respectively.

The SC orbitals in the chair and boat TSs can be obtained from the SU orbitals depicted in Figs. 3 and 4 through symmetry operations of the C_{2h} and C_{2v} PSGs, respectively; thus in the chair TS, orbitals ϕ_1, ϕ_2, and ϕ_3 are equivalent to ϕ_6, ϕ_5, and ϕ_4 through $\hat{C}_2$ rotations. Also, orbitals ϕ_1 and ϕ_6 are equivalent to orbitals ϕ_3 and ϕ_4 through reflections on the $\hat{\sigma}_h$ plane perpendicular to the $\hat{C}_2$ axis. In the boat TS, orbitals ϕ_1, ϕ_2, and ϕ_3 are equivalent to ϕ_6, ϕ_5, and ϕ_4 through $\hat{\sigma}_v$ reflections.

As regards to the chair TS SC orbitals, the distortion of ϕ_1 in the z direction towards ϕ_6, which is on the opposite allyl fragment, and its distortion towards ϕ_2 in the same allyl fragment is noticeable. The same type of distortion is observed in ϕ_2 which is shown in Fig. 3b, and is equivalent to ϕ_5 only. Here it is necessary to emphasize the similarity between ϕ_μ ($\mu = 1$–6) in this chair conformation and the SC orbitals in benzene [26]. Table 1 shows the overlap integrals between the active orbitals from the SC(20c, 6v) wave function of the chair TS. Note the following relations:

$$\langle\phi_1|\phi_2\rangle = \langle\phi_2|\phi_3\rangle = \langle\phi_4|\phi_5\rangle = \langle\phi_5|\phi_6\rangle \approx \langle\phi_3|\phi_4\rangle = \langle\phi_1|\phi_6\rangle \ . \tag{3.8}$$

In other words, the nearest-neighbour overlaps are the same in each allylic fragment and, moreover, are very similar to the interallylic overlap integrals $\langle\phi_3|\phi_4\rangle = \langle\phi_1|\phi_6\rangle$. As shown in Table 1, these overlap integrals are large in comparison to the other integrals. Thus, one expects considerable interaction between nearest-neighbour electrons in the chair structure. A VB calculation at this chair TS using the SC wave function showed the following eigenvector:

$$\Psi_{VB} = R_1 + 0.20R_2 + 0.20R_3 + R_4 + 0.18R_5 \ , \tag{3.9}$$

hence showing an in-phase resonance between all structures. If one defines the resonance energy as the energy difference between Ψ_{VB} and one Kekulé structure (R_1 or R_4, see Fig. 2)

$$E_{RES} = E(\Psi_{VB}) - E(R_1), \tag{3.10}$$

then, since the energy of one Kekulé structure is $E(R_1) = -232.937\ 620$ hartree, the resonance energy is $E_{RES} = 85.4\ \text{kJ mol}^{-1}$ ($103.5\ \text{kJ mol}^{-1}$ if one includes the 170 remaining ionic structures – full VB). The resonance energy in benzene is $83.6\ \text{kJ mol}^{-1}$ ($103.2\ \text{kJ mol}^{-1}$ in the full-VB calculation)[1]. The spin weights (in percent) of Ψ_{VB} are shown in the first row of Table 3: $W_1 = W_4 = 40.1$, $W_2 = W_3 = 6.8$, and $W_5 = 6.2$.

[1] Using an SC(18c, 6v) wave function and the 6-31G** basis set, which contains additional polarization p functions on the hydrogens

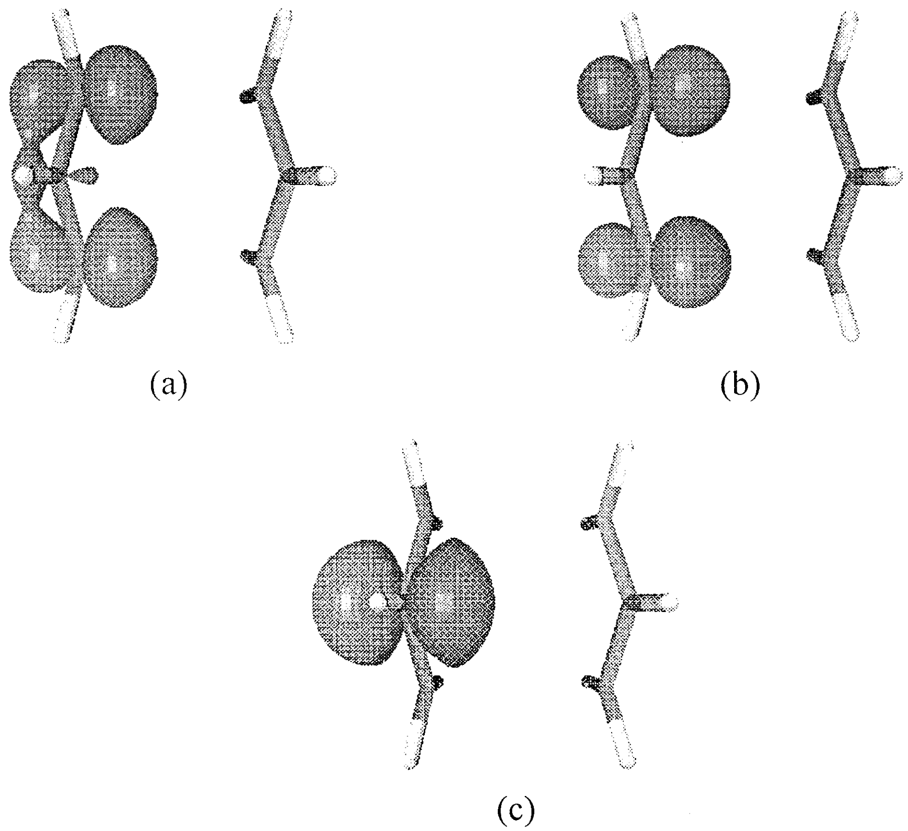

Fig. 4a–c. Symmetry-unique SC orbitals in the C_{2v} boat transition structure using a SC(20c, 6v)/6-31G* wave function with the optimized geometry at the CAS(6,6)/6-31G* level of theory. **a** Orbital ϕ_1 (symmetry-equivalent to ϕ_4); **b** orbital ϕ_2 (symmetry-equivalent to ϕ_5); **c** orbital ϕ_3 (symmetry-equivalent to ϕ_6)

Table 1. Overlap integrals between active orbitals in the C_{2h} chair transition structure (*TS*) from SC(20c, 6v) calculations using the 6-31G* basis set and the geometry shown in Fig. 1a

	ϕ_1	ϕ_2	ϕ_3	ϕ_4	ϕ_5	ϕ_6
ϕ_1	1	0.5203	0.0742	−0.0959	0.0806	0.5196
ϕ_2		1	0.5203	0.0806	−0.0968	0.0806
ϕ_3			1	0.5196	0.0806	−0.0959
ϕ_4				1	0.5203	0.0742
ϕ_5					1	0.5203
ϕ_6						1

Table 2. Overlap integrals between active orbitals in the C_{2v} boat TS from SC(20c, 6v) calculations using the 6-31G* basis set and the geometry shown in Fig. 1b

	ϕ_1	ϕ_2	ϕ_3	ϕ_4	ϕ_5	ϕ_6
ϕ_1	1	0.0000	0.7347	0.2518	0.0000	0.1383
ϕ_2		1	0.0000	0.0000	0.4784	0.0000
ϕ_3			1	0.1383	0.0000	0.1020
ϕ_4				1	0.0000	0.7347
ϕ_5					1	0.0000
ϕ_6						1

These weights are also very similar to those for benzene [26] ($W_1 = W_4 = 40.3$, $W_2 = W_3 = W_5 = 6.5$).

The second root of the VB calculation in the chair TS, which corresponds to the valence state ^1A_u, lies at 4.81 eV (4.93 eV in the full-VB calculation) above the ground state and is described by R_1–R_4, i.e., an out-of-phase combination of the two Kekulé structures. This state bears a striking resemblance to the first valence excited state in benzene, $^1B_{2u}$, which lies experimentally at 4.90 eV above the ground state, and is also described by K_1–K_2 [27]. At this point it should be emphasized that the aromaticity of the chair TS was already manifested in the work of Kozlowski et al. [12].

Turning now to the boat TS, the shapes of ϕ_1 and ϕ_2 are to be contrasted with those of the chair TS (Fig. 3). Thus, these orbitals do not have a localized pattern compared to the chair solution, but a semilocalized nature characterized by in-phase $\phi_1^{\text{boat}} \approx \phi_1^{\text{chair}} + \phi_3^{\text{chair}}$ and out-of-phase $\phi_2^{\text{boat}} \approx \phi_1^{\text{chair}} - \phi_3^{\text{chair}}$ combinations; however, orbital ϕ_3 in Fig. 4c (localized on the central carbon in the allyl fragment) has a similar shape compared to ϕ_2 in the chair (Fig. 3b). Table 2 shows the overlap integrals between the active orbitals from the SC(20c, 6v) wave function of the boat TS. The overlap integrals $\langle\phi_1|\phi_2\rangle$ and $\langle\phi_2|\phi_3\rangle$ are exactly zero due to the symmetry properties of the wave function. Thus, if we consider only one allylic fragment[2], ϕ_1 and ϕ_3 belong to the b_1 irreducible representation (irrep), and ϕ_2 to the a_2 irrep of C_{2v}. The same results from ϕ_4 and ϕ_6 (b_1) and ϕ_5 (a_2) on the opposite allylic fragment. As stated earlier, the main difference between the chair and boat TSs

[2]As an approximation we consider that each allyl in the boat TS has C_{2v} symmetry. Strictly speaking they have C_S symmetry

Table 3. Spin-only Rumer weights (W_i, i = 1–5) for the chair and boat TSs in the Cope rearrangement using the SC(20c, 6v) wave function and the 6-31G* basis set, at different optimized geometries. Values are given in percent, $\sum_{i=1}^{5} W_i = 100$. The interallylic distance R_1 is given in angstrom

Model geometries	Structure	Solution	R_1	W_1	W_2	W_3	W_4	W_5
CAS(6,6)	Chair	Localized	2.192	40.09	6.83	6.83	40.09	6.17
CASPT2[a]	Chair	Localized	1.745	11.85	0.86	0.86	11.85	74.58
MP4(SDQ)	Chair	Localized	1.851	17.81	3.16	3.16	17.81	58.08
QCISD	Chair	Localized	1.871	18.40	3.62	3.62	18.40	55.95
CAS(6,6)	Boat	Antipair	2.545	5.34	89.56	−0.11	5.35	−0.15
CASPT2[a]	Boat	Localized	2.139	39.27	6.90	6.90	39.27	7.66
MP4(SDQ)	Boat	Localized	2.139	39.30	7.26	7.26	39.30	6.89
QCISD	Boat	Localized	2.154	39.25	7.67	7.67	39.25	6.15

[a] Optimized geometries at the CAS(6,6)/6-31G* level with R_1 constant (see text)

Table 4. Self-consistent field (*SCF*), complete-active space (*CAS*) SCF and SC energies (in atomic units) for the chair and boat TSs in the Cope rearrangement, using the 6-31G* basis set. The interallylic distance (R_1) is given in angstrom

Structure	R_1	SCF	CAS	SC
Chair	2.192	−232.890 262	−232.977 134	−232.970 163
Chair	1.745 (fixed)	−232.874 475	−232.978 362	−232.975 714
Boat	2.545	−232.868 456	−232.970 005	−232.965 696
Boat	2.139 (fixed)	−232.876 716	−232.965 165	−232.958 145

Table 5. Overlap integrals between active orbitals in the C_{2h} chair TS from SC(20c, 6v) calculations using the CAS(6,6)/6-31G* optimized geometry fixing R_1^{chair} to 1.745 Å

	ϕ_1	ϕ_2	ϕ_3	ϕ_4	ϕ_5	ϕ_6
ϕ_1	1	0.2674	0.0673	0.0613	0.1342	0.7853
ϕ_2		1	0.2674	0.1342	−0.1984	0.1342
ϕ_3			1	0.7853	0.1342	0.0613
ϕ_4				1	0.2674	0.0673
ϕ_5					1	0.2674
ϕ_6						1

Table 6. Overlap integrals between active orbitals in the C_{2v} boat TS from SC(20c, 6v) calculations using the CAS(6,6)/6-31G* optimized geometry fixing R_1^{boat} to 2.139 Å

	ϕ_1	ϕ_2	ϕ_3	ϕ_4	ϕ_5	ϕ_6
ϕ_1	1	0.5055	0.0574	−0.0987	0.0917	0.5496
ϕ_2		1	0.5055	0.0917	−0.0675	0.0917
ϕ_3			1	0.5496	0.0917	−0.0987
ϕ_4				1	0.5055	0.0574
ϕ_5					1	0.5055
ϕ_6						1

stems from the distance between the allylic fragments: $R_1^{\text{chair}} = 2.192$ Å and $R_1^{\text{boat}} = 2.545$ Å. This difference provides a different electronic structure for either structure, as shown by the shapes of the orbitals. Thus, the chair SC wave function provides a localized orbital centred on each carbon atom, reminiscent of the SC orbitals in the benzene molecule. This is to be contrasted with the boat structure since its SC wave function resembles closely that of two weakly interacting allyl radicals, as shown by the overlap integrals (Table 2) and the shapes of the orbitals (Fig. 4). Moreover, the overlap integral $\langle\phi_1|\phi_3\rangle = 0.735$ in the boat structure is very similar to the overlap integral $\langle\pi_{b_1}|\pi'_{b_1}\rangle$ of the (ground state) antipair solution of the allyl radical [28]. As shown in Table 4, the SC wave function recovers 92 and 96% of the nondynamical correlation energy from the CASSCF wave function for the chair and boat structures, respectively.

It has recently been shown that inclusion of dynamical correlation in the Cope rearrangement is important in order to obtain a single TS on the potential energy hypersurface (PEH). As mentioned in the Introduction, Hrovat et al. [9] performed CASSCF and CASPT2 (second-order perturbative expansion in which the reference wavefunction is of CASSCF type) calculations and showed that at the CASPT2 level only single stationary points of C_{2h} and C_{2v} symmetry were found for the chair and the boat geometries, respectively. They performed single-point energy calculations at the CASPT2/6-31G* level along slices of the PEH maintaining the C_{2h} and C_{2v} symmetries and varying the interallylic distance R_1 (Fig. 1). The geometry of every point was optimized at the CAS(6,6)/6-31G* level of theory. Thus, they give $R_1^{\text{chair}} = 1.745$ Å and $R_1^{\text{boat}} = 2.139$ Å for the "optimized" geometries of the chair and boat TSs at CASPT2/6-31G* level, respectively.

Following Hrovat et al. [9], we performed geometry optimizations at the CAS(6,6)/6-31G* level maintaining the C_{2h} and C_{2v} symmetry at the R_1 distance found in their CASPT2 calculations. SC calculations were then performed at these geometries using the same wave function with six active electrons: SC(20c, 6v). The overlap integrals between the six active orbitals from the SC(20c, 6v) calculations using the above chair and boat geometries are given in Tables 5 and 6, respectively.

Figures 5 and 6 depict the converged SU SC orbitals from the SC(20c, 6v) wave function in the chair and boat structures, respectively, using the CAS(6,6)/6-31G* optimized geometries at $R_1^{\text{chair}} = 1.745$ Å and $R_1^{\text{boat}} =$

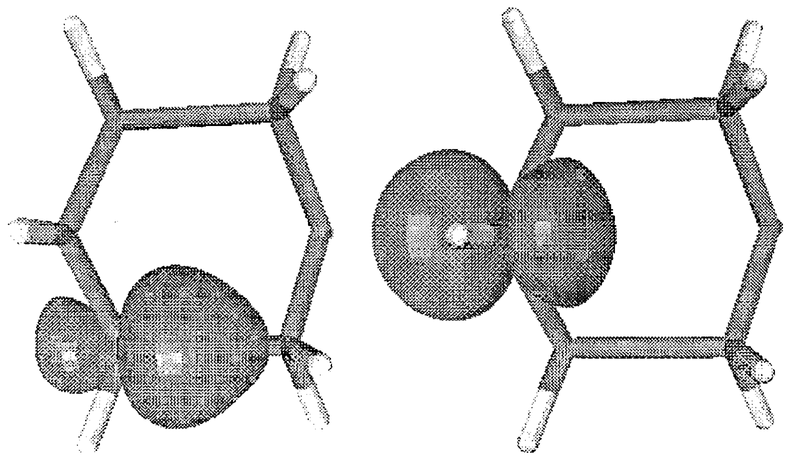

(a) (b)

Fig. 5a, b. Symmetry-unique SC orbitals in the C_{2h} chair transition structure using a SC(20c, 6v) wave function with the optimized geometry at the CAS(6,6)/6-31G* level of theory with a fixed interallylic distance of $R_1^{\mathrm{chair}} = 1.745$

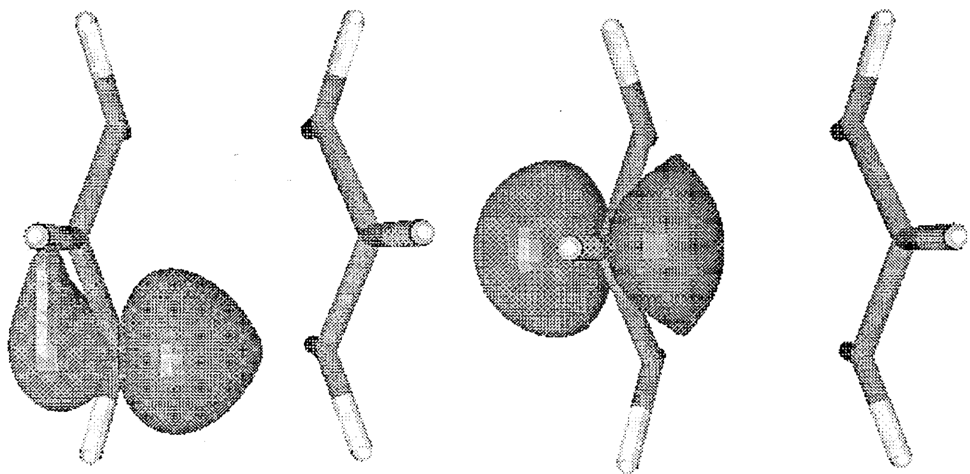

(a) (b)

Fig. 6a, b. Symmetry-unique SC orbitals in the C_{2v} boat transition structure using a SC(20c, 6v)/6-31G* wave function with the optimized geometry at the CAS(6,6)/6-31G* level of theory with a fixed interallylic distance of $R_1^{\mathrm{boat}} = 2.139$ Å

2.139 Å, respectively. The Rumer weights using the SC(20c, 6v) wave functions of the chair and boat structures at the different geometries are given in Table 3.

As shown in Table 5 and in Fig. 5, the chair TS now shows a diradical structure: this can be seen from the smaller overlap between the neighbour orbitals on each allyl fragment $\langle\phi_1|\phi_2\rangle = 0.27$ (and the equivalent counterparts) and by the shape of the SC orbitals in Fig. 5, which have smaller distortions towards their neighbours. Because the interallylic distance is now reduced to $R_1^{\mathrm{chair}} = 1.745$, the interfragment overlap integrals $\langle\phi_1|\phi_6\rangle = \langle\phi_3|\phi_4\rangle = 0.79$ are larger than those from the chair TS CAS optimized geometry (see Table 1: $\langle\phi_1|\phi_6\rangle = \langle\phi_3|\phi_4\rangle = 0.52$). Figure 5 shows the SU SC orbitals in this chair TS. It is obvious from the shape of these orbitals that there is a smaller overlap between them compared to the CAS chair TS. Moreover, Fig. 5b shows a big lobe for ϕ_2 in the outer direction of the allyl fragment, hence characterizing an almost "isolated" electron. Since there is one such electron on the other allyl fragment, it is clear that this chair TS corresponds to a diradical. The percentage of diradical character is W_5 ~75%, as shown in the second row of Table 3.

Curiously, the boat TS with $R_1^{\mathrm{boat}} = 2.139$ Å now appears to have aromatic character as shown by the overlap integrals and the distortions of the SU SC orbitals from Table 6 and Fig. 6, respectively (compare the overlap integrals from Table 6 with those from Table 1).

Finally, TS optimizations of the chair and boat conformations at the MP4(SDQ)/6-31G* (fourth-order Møller-Plesset perturbation theory with single, double and quadruple substitutions) and QCISD/6-31G* (quadratic configuration interaction with single and double substitutions) level of theory were then performed. These are the models within the suite of programs Gaussian94 [23] that allow analytical gradients of the energy with respect to nuclear displacements. The interallylic distances in the MP4(SDQ) and QCISD TSs are also gathered in Table 3. As in the above cases, we performed SC calculations on the MP4(SDQ) and QCISD TS geometries, using the SC(20c, 6v) wave function. For the boat TS, the CASVB code [29], which is implemented in the suite of programs MOLPRO [30], was used in the MP4(SDQ) and QCISD TS optimized geometries due to convergence problems in the SC wave function. The Rumer weights from these SC wave functions are also shown in Table 3.

As shown in Table 3, the chair MP4(SDQ) and QCISD TS optimized geometries have a similar interallylic distance: 1.851 and 1.871 Å respectively; however, the diradical character is now reduced to about 56%. This is reasonable since these distances are slightly larger than the CASPT2 one (1.745 Å). As far as the boat TS is concerned, the MP4(SDQ) and QCISD TSs also show aromatic character and similar interallylic distances (2.139 and 2.154 Å) compared to the CASPT2 one (2.139 Å).

4 Conclusions

In this work we have shown that SC theory features an aromatic or a diradical-dominating character in the C_{2h} chair TS of the Cope rearrangement depending on whether one uses the TS optimized geometry in a wave function including nondynamical or dynamical correlation energy, respectively. In the case of the boat TS, these features are different: application of SC theory to optimized TS geometries with nondynamical or dynamical wave functions show allylic or aromatic character, respectively. There is, however, a common interallylic distance ($R_1 \sim 2.15$–2.20) where the SC wave function shows aromaticity in the chair and boat TS.

It is clear from these results that the SC wave function does not show whether the Cope rearrangement of 1,5-hexadiene passes through an aromatic or a diradical TS, due to the limitations of the one-configuration (of singly occupied orbitals) approximation; however, it gives an interesting interpretation of the aromatic–diradical character of different TSs as a function of the interallylic distance. Our next goal is to perform constrained SC calculations along slices of the C_{2h} chair and C_{2v} boat surfaces in order to see the fraction of diradical versus aromatic character along the interallylic distance R_1[3].

Acknowledgements. The author is indebted to the late Dr. Joseph Gerratt for many interesting discussions. D.L. Cooper is acknowledged for his CASVB calculations on the MP4(SDQ) and QCISD optimized boat TS geometries. This work was supported by the TMR program of the European Community through project number ERBFMBICT97-2223.

[3] This can be done by imposing constraints in the spin-coupled wave function, and forcing allylic or localized wave functions along R_1

References

1. Dewar MJS, Jie C (1987) J Am Chem Soc 109: 5893
2. Dewar MJS, Jie C (1987) J Chem Soc Chem Commun 1451
3. Dewar MJS (1992) Int J Quantum Chem 44: 427
4. Dewar MJS, Healey EF (1987) Chem Phys Lett 141: 521
5. Osamura Y, Kato S, Morokuma K, Feller D, Davidson ER, Borden WT (1984) J Am Chem Soc 106: 3362
6. Morokuma K, Borden WT, Hrovat DA (1988) J Am Chem Soc 110: 4474
7. Hrovat DA, Borden WT, Vance RL, Rondan NG, Houk KN, Morokuma K (1990) J Am Chem Soc 112: 2018
8. Dupuis M, Murray C, Davidson ER (1991) J Am Chem Soc 113: 9756
9. Hrovat DA, Morokuma K, Borden WT (1994) J Am Chem Soc 116: 1072
10. Anderson K, Malmqvist P-A, Roos BO, Sadlej AJ, Wolinski K (1990) J Phys Chem 94: 5483
11. Anderson K, Malmqvist P-A, Roos BO (1992) J Chem Phys 96: 1218
12. Kozlowski PM, Dupuis M, Davidson ER (1995) J Am Chem Soc 117: 774
13. Jiao H, Schleyer PvR (1995) Angew Chem Int Ed Engl 34: 334
14. Kutzelnigg W, Fleischer U, Schindler M (1990) NMR Basic Princ Prog 23: 165
15. Gerratt J (1971) Adv At Mol Phys 7: 141
16. McNicholas SJ (1997) Ph.D. thesis. University of Bristol
17. Pauncz R (1979) In: *Spin eigenfunctions*, Plenum, New York, Plenum, 370p
18. Rumer G (1932) Göttingen Nachr 337
19. (a) Serber R (1934) Phys Rev 45: 461; (b) Serber R (1934) J Chem Phys 2: 697
20. Chirgwin BH, Coulson CA (1950) Proc R Soc Lond A 201: 196
21. Gallup GA, Norbeck JM (1973) Chem Phys Lett 21: 495
22. Gerratt J, Raimondi M (1980) Proc R Soc Lond A 371: 525
23. Frisch MJ, Trucks GW, Schlegel HB, Gill PMW, Johnson BG, Robb MA, Cheeseman JR, Keith T, Petersson GA, Montgomery JA, Raghavachari K, Al-Laham MA, Zakrzewski VG, Ortiz JV, Foresman JB, Cioslowski J, Stefanov BB, Nanayakkara A, Challacombe M, Peng CY, Ayala PY, Chen W, Wong MW, Andres JL, Replogle ES, Gomperts R, Martin RL, Fox DJ, Binkley JS, Defrees DJ, Baker J, Stewart JP, Head-Gordon M, Gonzalez C, and Pople JA (1995) Gaussian, Gaussian 94, revision E.1, Pittsburgh, Pa
24. Salem L (1982) Electrons in chemical reactions: first principles. Wiley, New York
25. Pipek J, Mezey PG (1989) J Chem Phys 90: 4916
26. Cooper DL, Gerratt J, Raimondi M (1986) Nature 323: 699
27. da Silva EC, Gerratt J, Cooper DL, Raimondi M (1994) J Chem Phys 101: 3866
28. Oliva JM, Gerratt J, Cooper DL, Karadakov PB, Raimondi M (1997) J Chem Phys 106: 3663
29. Thorsteinsson T, Cooper DL, Gerratt J, Karadakov PB, Raimondi M (1996) Theor Chim Acta 93: 343
30. Werner H-J, Knowles PJ, with contributions from Amos RD, Berning A, Cooper DL, Deegan MJO, Dobbyn AJ, Eckert F, Hampel C, Leininger T, Lindh R, Lloyd AW, Meyer W, Mura ME, Nicklaß A, Palmieri P, Peterson K, Pitzer R, Pulay P, Rauhut G, Schütz M, Stoll H, Stone AJ, Thorsteinsson T. MOLPRO a package of ab initio programs